



LAWRENCE
LIVERMORE
NATIONAL
LABORATORY

X-ray Thomson scattering as a temperature probe for gigabar shock experiments

T. Doeppner

November 5, 2013

The Twenty-Fourth Biennial International Conference of the International Association for the Advancement of High Pressure Science and Technology (AIRAPT)
Seattle, WA, United States
July 7, 2013 through July 12, 2013

Disclaimer

This document was prepared as an account of work sponsored by an agency of the United States government. Neither the United States government nor Lawrence Livermore National Security, LLC, nor any of their employees makes any warranty, expressed or implied, or assumes any legal liability or responsibility for the accuracy, completeness, or usefulness of any information, apparatus, product, or process disclosed, or represents that its use would not infringe privately owned rights. Reference herein to any specific commercial product, process, or service by trade name, trademark, manufacturer, or otherwise does not necessarily constitute or imply its endorsement, recommendation, or favoring by the United States government or Lawrence Livermore National Security, LLC. The views and opinions of authors expressed herein do not necessarily state or reflect those of the United States government or Lawrence Livermore National Security, LLC, and shall not be used for advertising or product endorsement purposes.

X-ray Thomson scattering as a temperature probe for Gbar shock experiments

T Döppner¹, A L Kritcher¹, S H Glenzer², B L Bachmann¹, D Chapman³, G W Collins¹, R W Falcone⁴, J Hawreliak¹, D Kraus⁴, O L Landen¹, H J Lee², S Le Pape¹, T Ma¹, P Neumayer⁵, R Redmer⁶ and D C Swift¹

¹Lawrence Livermore National Laboratory, Livermore, CA 94551, USA.

²SLAC National Accelerator Laboratory, Menlo Park, CA 94025, USA.

³AWE plc, Plasma Physics group, Aldermaston, Reading RG7 4PR, UK.

⁴Lawrence Berkeley National Laboratory, Berkeley, CA 94720, USA.

⁵Gesellschaft für Schwerionenphysik, Darmstadt, Germany.

⁶University of Rostock, 18051 Rostock, Germany.

E-mail: ¹doeppner1@llnl.gov

Abstract. In X-ray Thomson scattering (XRTS), spectrally-resolved spectrometry of probe x-rays scattered from matter gives an elastic (ionic) and an inelastic (electronic) feature, whose location, width, and amplitude can be analyzed for electron density and temperature. This diagnostic is complementary to traditional, mechanical EOS measurements which do not directly constrain temperature. XRTS has been demonstrated on planar dynamic-loading experiments at the Omega laser, and a spectrometer has been constructed for use at the National Ignition Facility (NIF). We plan to obtain XRTS measurements into the Gbar regime using hohlraum-driven converging shocks at NIF. In these experiments, the radial profile through the sample at any instant of time varies greatly, though the XRTS signal is dominated by the densest region, which is close to the shock front where simultaneous radiography obtains an EOS measurement.

1. Introduction

Matter at extreme pressures that approach and exceed 1 Gbar (=100 TPa) occurs widely in astrophysical objects such as giant planets [1, 2] and brown dwarfs, and inertial confinement fusion (ICF) plasmas [3]. Recent advances in experimental capabilities to produce high-energy-density plasmas using high-power lasers enables the creation of these astrophysically relevant conditions in the laboratory. Experimental measurements of the Equation of State (EOS) at such conditions are still scarce but of great importance for benchmarking dense matter modeling. We have proposed to use the National Ignition Facility (NIF) [4] to create extreme pressure (100 Mbar - \sim 1 Gbar) conditions in a convergent shock geometry and measure the EOS of CH plastic along the principal Hugoniot [5].

State-of-the-art EOS measurements provide the relation between pressure and compression by tracking the shock velocity when transiting from a reference material into the sample under study [6] or absolutely through radiography [7]. Information on temperature has to be separately obtained. Here, we propose to use x-ray Thomson scattering (XRTS) to measure the plasma temperature through the electron velocity distribution. XRTS has been developed to accurately

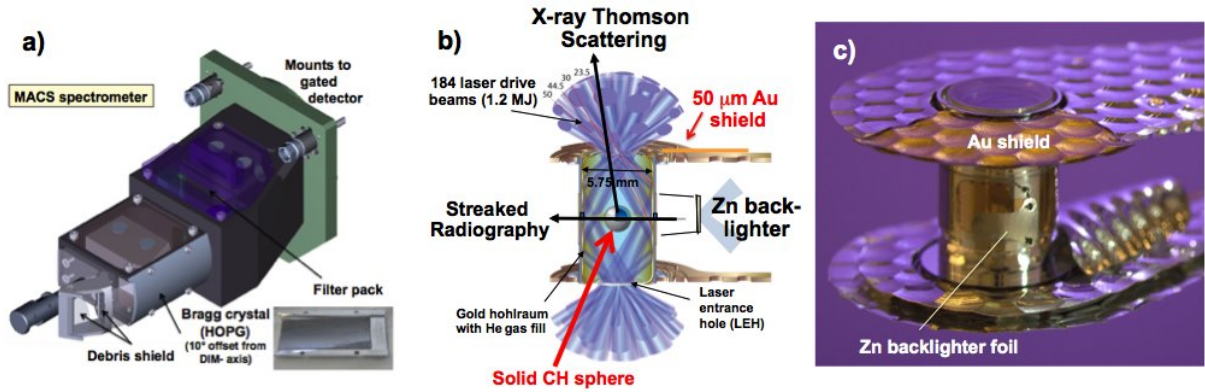


Figure 1. Schematic experimental configuration (b). The Mono angle crystal spectrometer (MACS) with cylindrically curved HOPG crystal (a) is mounted in the polar diagnostic port to measure x-ray Thomson scattering through the top laser entrance hole. (c) photograph of Gbar hohlraum target with view of zinc backlighter foil and dedicated gold shield for XRTS.

characterize plasma conditions at and above solid density in a series of experiments on the Omega laser at the Laboratory for Laser Energetics in Rochester, NY. While most experiments used directly-driven planar foils [10], first experiments demonstrated XRTS from spherical shell targets [9, 11] that took advantage of convergence effects to demonstrate characterization of electron densities as high as $n_e = 2 \times 10^{24} \text{ cm}^{-3}$ with x-ray Thomson scattering [9].

In this work we present the design considerations for the XRTS part of the NIF Gbar EOS experiments. After describing the experimental platform, we will give an overview of the spectrometer design and the strategy for background mitigation. The concluding section will discuss simulated scattering spectra for expected plasma conditions.

2. Experimental Configuration

Figure 1b gives an overview of the experimental platform. We are using hohlraum targets based on the 1D convergent ablator (1D ConA) target design developed during the National Ignition Campaign [12]. The 1D ConA platform is used to measure radiographs of the in-flight shell radii at and close to peak velocity in indirectly driven ICF implosions. We use the same, well-characterized Zn He $_{\alpha}$ backlighter at 9.0 keV as these ICF experiments with CH ablator. In contrast to the 1D ConA's our targets are fielded from the Cryo-Targetpositioner (at azimuthal angle $\phi = 5$). In this configuration the radiography line-of-sight is close to perpendicular to the target positioner and allows the backlighter foil to be mounted closer to the target (6 mm vs. 12 mm) which is beneficial for increasing the number of photons on the CH target. For comparison, the backlighter stand-off in typical Omega XRTS experiments is on order of 1 mm.

Our experiments use 9.45 mm long and 5.75 diameter gold hohlraums with a laser entrance hole (LEH) diameter of 3.37 mm. For the hohlraum drive we adapt pulse shapes from the ignition program that were optimized to provide good hohlraum radiation symmetry. Figure 2 shows the laser pulse that was chosen for the first NIF Gbar EOS experiment. A total of 184 beams in 46 quads with a total energy of 1.2 MJ at a wavelength of 351 nm are directed into the hohlraum to obtain radiation temperatures of up to 280 eV. The remaining 8 NIF beams from quads 26-bottom and 31-top are directed to the 5 μm thick Zn backlighter foil that is mounted at $\phi = 258.75^\circ$. The backlighter pulses have a picket to create a pre-plasma for enhanced x-ray conversion efficiency [13] which is followed by a delayed, 5 ns long main pulse defining the time-window over which radiography data will be recorded. The backlighter beams use regular

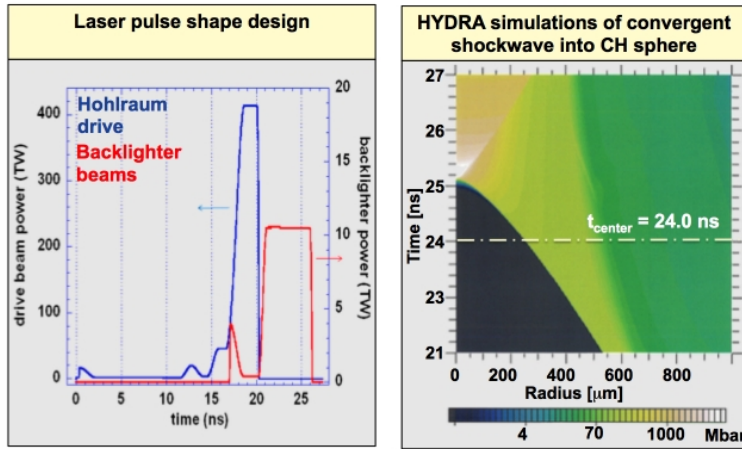


Figure 2. Laser pulse shapes (left) and pressure map inferred from hydrodynamic simulation (right). For more details see text and reference [5].

phase plates (projected spot size is ≈ 1.1 mm) and are pointed with a separation of 1.1 mm on the Zn foil to provide a uniform area backlighter beam profile. At peak power of 1.3 TW per beam we obtain intensities on order of 5×10^{14} W/cm², yielding a conversion efficiency into the Zn He- α line at 9.0 keV of 0.5% [13]. The hohlraum drive beams have four distinct shocks and are optimized to obtain a low-adiabat, high-convergence and high-symmetry implosion in fully integrated experiments using deuterium-tritium fusion fuel. In our experiment we use a solid CH sphere with an outer diameter of 2.2 mm. Here, all shock waves have merged into a single shock wave at a radius of ~ 800 μm . After that, the single shock wave is increasing in strength as $1/r$ as it is converging. Figure 2b is showing simulated pressures as function of radius and time. In this design, before shock stagnation we obtain pressures of up to 500 Mbar at radii $r \geq 150$ μm for which a measurement of the density jump at the shock front is possible. For more details on the simulations we refer the reader to reference [5]. In the remaining part of the paper we present design considerations for the XRTS measurement.

3. X-ray Spectrometer Design

Simultaneous to the radiography measurement, x rays scattered from the CH ball leaving the hohlraum through the top LEH are recorded with a high-efficiency, gated x-ray spectrometer snout mounted in the polar diagnostic insertion manipulator (DIM) of the NIF target chamber, cf. figure 1b. This Mono Angle Crystal spectrometer (MACS, cf. figure 1a) was specifically designed and built for this experimental campaign, for details cf. reference [14]. In brief, a 30 mm wide, cylindrically curved highly-oriented pyrolytic graphite (HOPG) crystal, known to have the highest integrated reflectivity at 9 keV ($R_{int} \sim 5$ mrad), with a radius-of-curvature $R_{curv} = 54$ mm, is placed at 250 mm from the target chamber center. The crystal is offset by 10° from the vertical target chamber axis. For current standard polar DIM rotation (hGXI or rGXD) the crystal is at an azimuthal angle of $\phi = 135^\circ$, yielding a compound scattering angle of $\theta = 84.7 \pm 2.0^\circ$. A 4-strip gated micro channel plate (MCP) detector (100 ps integration time) is placed perpendicularly oriented with respect to the HOPG crystal surface, at magnification $M = 1$ for the central energy of 8.6 keV, and covering a spectral range from 7.4 - 10.0 keV. The curved crystal is focusing all Bragg-reflected x rays to strip 2 (S2) of the MCP, cf. figure 3 for a simulated signal envelope. Since the detector can not be placed parallel to the crystal as required for von-Hámos geometry due space constraints in the DIM, the signal is de-focused towards the edges of the spectral range. The signal width at best spatial focus at ~ 8.6 keV is determined by the HOPG mosaicity $\gamma \sim 1.0^\circ$ to $\Delta x = 2R_{curv} \tan \gamma \approx 1.9$ mm. This corresponds

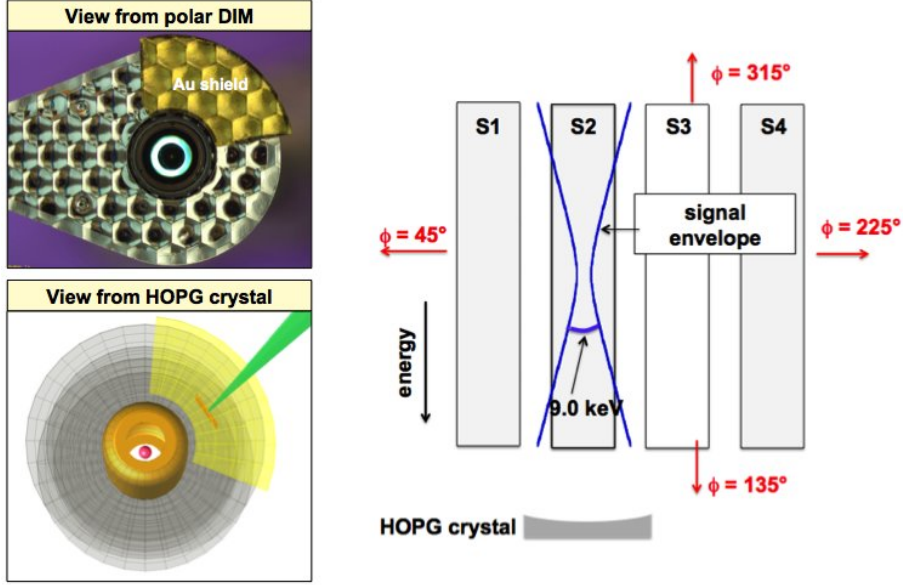


Figure 3. Polar view of 2.2 mm outer diameter CH ball (top left) and MACS field of view, 10° off the vertical NIF chamber axis, of the compressed plastic sphere at time of probing (bottom left). The curved MACS crystal focuses x rays are to the second strip (S2) of a 4-strip gated MCP detector (as seen from back of MCP towards target chamber center).

to the spatial spectrometer resolution in the non-dispersive direction. For future designs we will use HAPG (Highly Annealed Pyrolytic Graphite) coating which has 10x smaller mosaicity for improved spatial resolution at comparable peak reflectivity [15]. Additionally we are designing a conically curved crystal that will provide good focussing over the full spectral range. Despite its rather coarse spatial resolution in the current design the cylindrically curved HOPG allows to discriminate undesired background signals. In particular, we use this property to avoid any signal from the plasma plume originating from the backlighter foil onto strip 2 of the MCP detector. A $50 \mu\text{m}$ thick gold foil with residual transmission of 4×10^{-7} at 9 keV is used to block the direct line of sight between the Zn foil and the HOPG crystal. The Au foil extends to a radius of 10.2 mm from the central axis, i.e. 4.2 mm beyond the radial location of the Zn foil at $r = 6$ mm. The backlighter pointing is off by 33° from being mounted perpendicular to the spectral dispersion direction, hence emission from the Zn plasma plume extending beyond the gold shield would be separated from the CH ball scatter by $10.2 \text{ mm} \times \cos 33^\circ = 8.5 \text{ mm}$ towards strip S1 which is almost a full strip separation (9.35 mm).

4. X-ray Thomson scattering signals

The XRTS signal is described by the dynamic structure factor $S(\mathbf{k}, \omega)$ which can be decomposed into three main components [8]

$$S(\mathbf{k}, \omega) = W_R(k) + Z_f S_{ee}^o(\mathbf{k}, \omega) + Z_b \int S_{ce}(\mathbf{k}, \omega - \omega') S_s(\mathbf{k}, \omega') d\omega' \quad (1)$$

describing the near-elastic scattering ($W_R(k)$) from bound electrons, scattering from free electrons (S_{ee}^o), and inelastic scattering due to bound-free transitions. Contributions from the latter are negligible for the plasma conditions under consideration. Wunsch *et al.* showed in detail how $W_R(k)$ for a two-component plasma like CH can be calculated [16]. Z_f is the

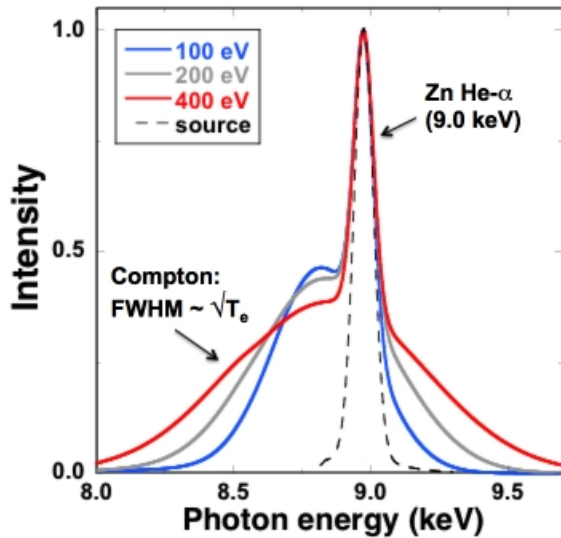


Figure 4. Simulated x-ray Thomson scattering spectra as function of electron temperature. Spectra are normalized to the elastic scattering peak. The instrument function is shown for comparison (dashed line). Spectra were simulated for $n_e = 1.5 \times 10^{24} \text{ cm}^{-3}$ and $Z_f^{(C)} = 6$.

ionization state and Z_b the number of bound electrons, respectively. Here, we restrict the discussion to $S_{ee}^o(\mathbf{k}, \omega)$, the electron–electron density correlation function. It describes the Compton scattering from free electrons which is down-shifted by $E_C = \hbar k^2/2m_e = 144 \text{ eV}$ (where $k = 2k_o \sin \theta = 6.1 \text{ \AA}^{-1}$) from the probe energy, and Doppler-broadened according to the velocity distribution of the electrons. While most of the previous Omega XRTS experiments were done in the near-degenerate regime ($n_e \sim 10^{24} \text{ cm}^{-3}$, $T_e \sim 10 \text{ eV}$) where the width of the Compton feature is mostly sensitive to the electron density n_e [8, 9, 11], the Gbar experiments reach temperatures up to 1 keV at 4 - 10 g/cm^{-3} , well into the non-degenerate regime. Here, the width of the Compton feature scales as $\text{FWHM}_{\text{Compton}} \propto \sqrt{T_e}$. While the Compton feature will not be sensitive to n_e , we will get mass density from the simultaneous radiography measurement and ionization Z_f from the ratio of the Rayleigh peak to the Compton peak. Figure 4 illustrates the temperature scaling in simulated XRTS spectra for the expected plasma conditions. Additionally, in the Gbar EOS experiments x-ray scattering occurs from an extended source ($d \sim 1 \text{ mm}$), sampling a range of plasma conditions. Accurate modeling of all relevant scattering and transport effects on the shape of the experimental spectrum is in progress [17].

In summary, we have designed and built a high-efficiency gated x-ray spectrometer for the NIF. By measuring the time-resolved x-ray Thomson scattering spectrum we will obtain information on temperature and ionization which will allow to further constrain the simultaneous absolute radiographic equation-of-state measurement in CH.

Acknowledgements

This work performed under the auspices of the U.S. Department of Energy by Lawrence Livermore National Laboratory under Contract DE-AC52-07NA27344 and supported by Laboratory Directed Research and Development Grant No. 11-ERD-050. RWF acknowledges support from SSAA program Contract No. DE-FG52-06NA26212. Special thanks go to Scott Burns and Allen house who designed and built the MACS spectrometer, and to Dan Kalantar, Tom McCarville and Reg Wood who worked out critically important alignment procedures.

References

- [1] Swift D C, Eggert J H, Hicks D G, Hamel S, Caspersen K, Schwegler E, Collins G W, Nettelmann N, and Ackland G J 2011 *Astrophys. J.* **744** 59

- [2] Stixrude L 2012 *Phys. Rev. Lett.* **108** 055505
- [3] Lindl J D, Amendt P, Berger R L, Glendinning S G, Glenzer S H, Haan S W, Kauffman R L, Landen O L, and Suter L J 2004 *Phys. Plasmas* **11** 339
- [4] Moses E I, Miller G H, and Wuest C R 2004 *Nuclear Fusion* **44** 228-238
- [5] Kritcher A L, Döppner T, Swift D C, Hawreliak J, Glenzer S H, Collins G W, Felker S, Landen O L, Lee H L, Rothman S, Chapman D, Thomas C, Jones O, Hammer J, Keane C, and Falcone R W 2013 *submitted to High Energy Density Physics*, 2013.
- [6] Barrios M A, Hicks D G, Boehly T R, Fratanduono D E, Eggert J H, Celliers P M, Collins G W, and Meyerhofer D D 2010 *Phys. Plasmas* **17** 056307
- [7] Cauble R, Perry T S, Bach D R, Budil K S, Hammel B A, Collins G W, Gold D M, Dunn J, Celliers P, and Da Silva L B 1998 *Phys. Rev. Lett.* **80** 1248
- [8] Glenzer S H and Redmer R 2009 *Rev. Mod. Phys.* **81** 1625
- [9] Kritcher A L, Döppner T, Fortmann C, Ma T, Landen O L, Wallace R, and Glenzer S H 2011 *Phys. Rev. Lett.* **107** 015002
- [10] Ma T, Döppner T, Falcone R W, Fletcher L, Fortmann C, Gericke D O, Landen O L, Lee H J, Pak A, Vorberger J, Wünsch K, and Glenzer S H 2013 *Phys. Rev. Lett.* **110** 065001
- [11] Fletcher L B, Kritcher A L, Pak A, Ma T, Döppner T, Fortmann C, Divol L, Landen O L, Vorberger J, Chapman D A, Gericke D O, Falcone R W, and Glenzer S H 2013 *Phys. Plasmas*, **20** 056316
- [12] Hicks D G et al. 2012 *Phys. Plasmas*, **19** 122702
- [13] Barrios M A, Fournier K B, Regan S P, Landen O L, May M, Opachich Y P, Widmann W, Bradley D K, and Collins G W 2013 *High Energy Dens. Phys.* **9** 626
- [14] Döppner T, Kritcher A L, Neumayer P, House A, Burns S, Glenzer S H, Landen O L, and Bell P 2014 High-efficiency time-resolving x-ray spectrometer for the National Ignition Facility. *submitted to Journal of Instrumentation*
- [15] Zastra U, Woldegeorgis A, Förster E, Loetzsch R, Marschner H, and Uschmann I 2013 *J. Instrum.*, **8** P10006
- [16] K Wünsch, J Vorberger, G Gregori, and D O Gericke. 2011 *Europhys. Lett.* **94** 25001
- [17] Chapman D, Döppner T, Kritcher A L, Bachmann B L, Glenzer S H, Hawreliak J, Kraus D, Landen O L, Swift D C, and Falcone R W 2014 Simulating x-ray Thomson scattering from high-density, millimeter-scale plasmas. *in preparation*